energies

MDPI

Article

Oxidation Kinetics of Neat Methyl Oleate and as a Blend with Solketal

Julian Türck [1,*], Fabian Schmitt [2], Lukas Anthofer [2], Anne Lichtinger [3], Ralf Türck [2,4], Wolfgang Ruck [1] and Jürgen Krahl [4,5]

[1] School of Sustainability, Leuphana Universität Lüneburg, Universitätsallee 1, 21335 Lüneburg, Germany
[2] Tecosol GmbH, Jahnstraße 2, 97199 Ochsenfurt, Germany
[3] Institute of Technical and Macromolecular Chemistry, Universität Hamburg, Bundesstraße 45, 20146 Hamburg, Germany
[4] Fuels Joint Research Group, Masch 16, 38531 Röttgesbüttel, Germany
[5] Innovation Campus Lemgo, OWL University of Applied Sciences and Arts, Campusallee 12, 32657 Lemgo, Germany
* Correspondence: julian.tuerck@stud.leuphana.de; Tel.: +49-9331-981522

Abstract: The complexity of biodiesel aging has shown that the mechanism needs further research. The rate of aging product formation and associated interactions can help improve fuel quality. Since biodiesel is a multicomponent system and constant changes occur in the chemical environment, which interactions yield which products must be shown in more detail. Particularly under observation was the correlation between peroxides and epoxides. In addition, it is critical that the influence and interactions of new drop-in fuel candidates be investigated. In this work, the kinetics of the formation of aging products of methyl oleate (C18:1) are studied. The aim was to reduce the complexity in order to be able to make more precise and detailed statements about the mechanism. Ketones, acids, peroxide, and epoxide values were recorded. A distinction is made between pure methyl oleate and mixtures with 3 wt% isopropylidene glycerine (solketal). After solketal decomposed in the blends, the aging process showed changes. The influence of solketal resulted in a higher number of acids and epoxides over time. It implied that peroxides are not necessarily the precursor of epoxides. In summary, correlation and solketal's influence showed that a sequence of aging products could be detected.

Keywords: oxidation kinetics; biodiesel aging; methyl oleate; solketal; alcohol influence; sequence of aging products

check for updates

Citation: Türck, J.; Schmitt, F.; Anthofer, L.; Lichtinger, A.; Türck, R.; Ruck, W.; Krahl, J. Oxidation Kinetics of Neat Methyl Oleate and as a Blend with Solketal. *Energies* **2023**, *16*, 3253. https://doi.org/10.3390/en16073253

Academic Editors: Vincenzo Motola, Reeta Goel and Neeta Sharma

Received: 3 March 2023
Revised: 2 April 2023
Accepted: 3 April 2023
Published: 5 April 2023

Copyright: © 2023 by the authors. Licensee MDPI, Basel, Switzerland. This article is an open access article distributed under the terms and conditions of the Creative Commons Attribution (CC BY) license (https://creativecommons.org/licenses/by/4.0/).

1. Introduction

As an already established fuel, biodiesel can help increase the regenerative capacity and sustainability of liquid chemical fuels. It can also reduce dependence on fossil fuels. Biodiesel is a multi-component system of fatty acid methyl esters that can be produced from various feedstocks (e.g., vegetable oils, fatty acids, etc.). Regardless of the feedstock used, methyl oleate is one of the most abundant fatty acids in biodiesel [1]. Methyl oleate has a double bond and is less reactive when compared with polyunsaturated components [2]. This reactivity can lead to fuel aging, which is an important factor that prevents an increase in miscibility. Fuel aging is the change in the physical and chemical properties of the fuel [3]. It starts with autoxidation, which means that oxygen is introduced into the unsaturated bonds of the fatty acid. As a result, the polarity of the fuel increases. Further effects on polarity result from the oligomerization of biodiesel that takes place during fuel aging [4,5]. Since fossil diesel fuels are comparatively nonpolar, this can lead to blending gaps. In addition, polar aging products exhibit enhancement of mutagenic emissions [6]. The process of oxygen incorporation occurs through peroxidation, known as lipid peroxidation [7], which also plays an important role on vegetable oils in food science [8,9]. In general, the initiation

of peroxidation can be started in different ways. A distinction can be made between heat with O_2, transition metallic ion traces, UV light, or traces of peroxides present [10]. With regard to oxygen, a distinction can be made between peroxidation using triplet and singlet oxygen [11]. Classical peroxidation with oxygen is carried out using triplet oxygen, which reacts with a radical of the biodiesel [12]. Nevertheless, the vegetable oil literature shows that singlet oxygen and the associated Schenck–Ene reaction can occur during oil rancidity [13]. Triplet-oxygen-based peroxidation starts with a radical, which is formed by allylic and bis-allylic components, which have a lower C-H bond dissociation energy [14]. Moreover, the radicals of these components are stabilized by further double bonds and thus, by mesomeric boundary formulas. Peroxidation with singlet oxygen occurs mostly by photocatalysis and has not played a role in the biodiesel aging literature. Since the spin transition follows an energetic excitation, other energy sources, such as thermal energy, are conceivable [15]. The decay of peroxides subsequently induces the radical mechanism of autoxidation. Figure 1 describes the main radical steps [16].

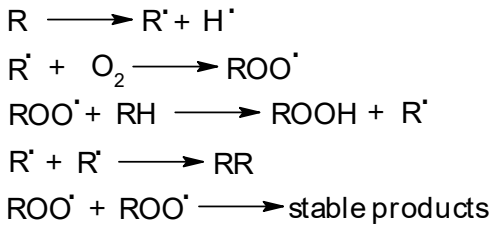

Figure 1. Main radical steps of autoxidation of lipids and biodiesel.

This decomposition produces the known aging products of biodiesel, namely carboxylic acids, aldehydes, ketones, etc. [17]. The key factor for stability of the fuel is how fast the aging proceeds. Therefore, the kinetics of aging and the associated sequence of the formation of aging products is crucial. The formation of the aging products and the associated reactivity of these components leads to increased aging behavior of the fuel. To increase the stability of the fuel, the radical aging mechanism is slowed down with the help of antioxidants (radical scavengers) [18]. Therefore, commercial radical scavengers, such as tert-butylhydroquinones (TBHQ), are used as additives in biodiesel [19]. In addition, other molecules, such as solketal, showed oligomerization-inhibiting behavior, although they are not applied as antioxidants [20]. Gel permeation chromatography (GPC) measurements showed that fewer higher molecular weight molecules are formed in the presence of solketal. The preparation of solketal is shown in Figure 2.

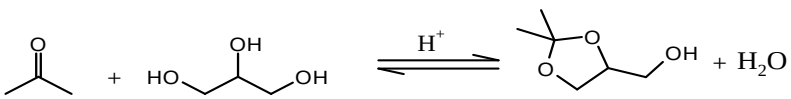

Figure 2. Proton-catalyzed condensation reaction of acetone and glycerol to produce solketal.

Solketal is produced from glycerin by means of a proton-based condensation reaction. It exhibits both alcohol and ketal functionality. In terms of fuel properties, solketal showed interesting properties in gasoline as it increases anti-knock properties [21]. In addition, more polar properties and a lower carbon chain length of fossil gasoline allow for higher blending capability. Furthermore, alcohols are also interesting drop-in components for diesel fuel. They increase the regeneration capacity of the diesel fuel while simultaneously increasing the molecular oxygen density. The lower number of C-C bonds and the absence of double bonds results in cleaner combustion with less soot formation [22]. However, the improvement in anti-knock properties is accompanied by a decrease in cetane number [23]. In addition, solketal has a relatively low heating value, which can lead to driving range problems [24]. Considering the properties of solketal, it is reasonable to blend solketal in

the lower percentage range (1–5% by volume). Before solketal can be used as a sustainable drop-in fuel, it is important to study the interaction of solketal with other fuel components.

The objective of this work is to investigate the influence of solketal on a monounsaturated biodiesel component using C18:1 as an example. The complex system of biodiesel aging is simplified by using pure methyl oleate. This is to observe the direct interaction of solketal with the double bond, as this site can be a starting point for aging. In addition, the kinetics of the formation and degradation of aging products will be studied in more detail.

2. Materials and Methods

2.1. Chemicals

The used chemicals were purchased from Merck KGaAA, Gernsheim, Germany. These were methyl oleate (C18:1, purity 99%) and solketal (purity 98%). The reference biodiesel was a rapeseed oil methyl ester (RME) delivered by Tecosol GmbH, Ochsenfurt, Germany. The water content of the chemicals was 100–200 ppm.

2.2. Fuel Aging

The experimental setup for the kinetics study was performed using a Metrohm 743 Rancimat instrument (Herisau, Switzerland). The blends were aged in 10-h increments up to 100 h. The physical parameters were set at a temperature of 110 °C with an air flow rate of 166.7 mL/min. The measurement setup was in accordance with EN 14112 (Figure 3) [25], so that the conductivity of the low-boiling decomposition products could be measured in the eluate vessel filled with distilled water (50 mL). The long reaction vessels were used and filled with 20 g of the sample. The solketal blends exhibited an amount of 3 wt% (600 mg). The range of the water content after aging was constantly between 0.1 and 0.2%.

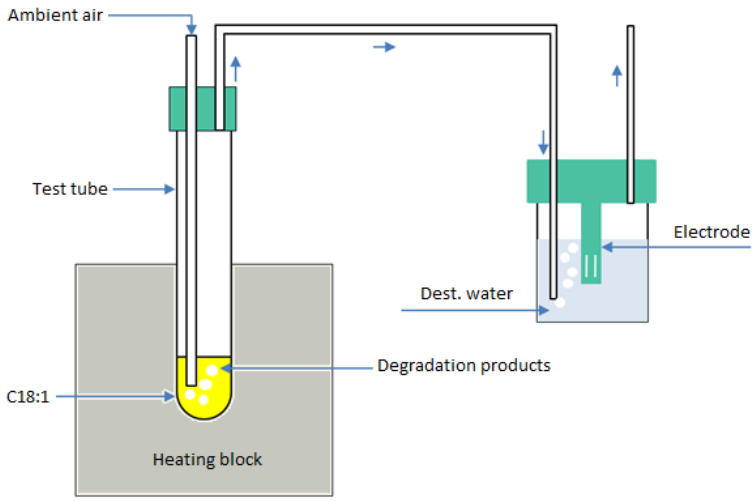

Figure 3. Schematic illustration of the experimental set-up (rancimate) according to DIN EN 14112.

2.3. Kinematic Viscosity

The kinematic viscosity was measured with a Stabinger viscometer from Anton Paar, Ashland, VA, USA, (SVM 3001) at 40 °C. The kinematic viscosity can be considered as an indicator of fuel aging. It is the result of the polymerization of biodiesel components, which results in stronger intermolecular interactions. Table 1 describes the kinematic viscosity of the chemicals used in the unaged and pure state.

Table 1. Kinematic viscosity at 40 °C for the pure chemicals.

	Kin. Viscosity [mm^2/s]
Methyl oleate	4.5
Solketal	5.1

2.4. Acid Value

The acid value describes the number of molecules with acidic functionality (e.g., carboxylic acid, sulfonic acid, etc.). The experimental setup was performed according to EN 14104 [26]. The method is based on automated potentiometric titration using an instrument from Metrohm, Herisau, Switzerland. During oxidative aging, acids and aging products of biodiesel are generated. Methanolic potassium hydroxide (KOH) was used as a titrant to determine the quantitative number of acids (c = 0.5 mol/L). Equation (1) describes the formula used to calculate acid value. The molar mass of KOH is expressed as 56.1; V is the consumption of KOH. The weight of the sample used was 1 g.

$$\mathrm{TAN} = \frac{56.1 \times \mathrm{V} \times \mathrm{c}}{\mathrm{m}} \quad (1)$$

2.5. Peroxide Value

Similarly to the determination of the acid value, the peroxide value was also measured by titration. In contrast to the acid value, the content was determined by classical titration according to Wheeler (EN ISO 3960) [27]. Peroxides are also a class of aging products and are quantified by this parameter. The peroxide value was determined as a function of the expected number of peroxides. A sample size of 200 mg was used for the kinetic experiment. The sample was dissolved in isooctane (40 mL) and glacial acetic acid (60 mL). Quantification was performed by oxidation of iodide anions. Potassium iodide (0.5 mL) was selected as the iodide source and added to the solution. The peroxides act as oxidizing agents. After the solution was homogenized, 100 mL of distilled water and 0.5 mL of starch solution (c = 10 g/L) were added to give the purple color of the iodine–starch complex. Sodium thiosulfate (c = 0.01 mol/L) was used as a titrant until the solution visually decolorized. The peroxide value (POV) can be determined using Equation (2).

$$\mathrm{POV} = \frac{(\mathrm{V} - \mathrm{V_0}) \times \mathrm{c} \times \mathrm{F} \times 1000}{\mathrm{m}} \quad (2)$$

2.6. Gas Chromatography with Mass Spectrometry (GC-MS)

GC–MS measurements were recorded using a Shimadzu gas chromatograph coupled with a mass spectrometer (GC = GC2030 and MS = GCMS QP2020 NX). The NIST20 library was chosen as the comparison database. The method chosen is a specific method for the detection of biodiesel-based molecules, which include the aging products. This experimental setup was used for the quantification of epoxides and ketones. To evaluate the yield of the aging products, the integrated peak areas were related to the areas of C18:1 in the unaged state. For sample preparation, 250 mg was dissolved in 5 mL of CS_2. Helium was run as the mobile phase. An SPL injector was also used. Table 2 describes the operating parameters.

Table 2. GC-MS operating parameter for the determination of epoxides and ketones.

GC:				
Temperature Program			**Column**	
Start temp.: 60 °C for 3 min			Dimension: 30.0 m × 0.25 mm × 0.20 µm	
Heating rate: 10.0 K/min			Type: Phenomenex ZB-FAME	
Finale temp.: 250 °C for 10 min			Max. temp.: 280 °C	
Total run time: 32 min				
Injector temp.: 250 °C				
Pressure [kPa]	Total Flow [mL/min]	Split Ratio	Column Flow [mL/min]	Injection Volume [µL]
72.9	64.5	1:50	1.21	1.0
MS:				
Ion Source Temperature			200 °C	
Interface Temperature			250 °C	
Ionization mode			Electron Ionization	
Scan mode			Total Ion Count	
m/z			20.00–600.00	

3. Results and Discussion

A first indication of change in the aging kinetics of methyl oleate and tsolketal blends compared with conventional biodiesel was obtained from recording the conductivity of the rancimate eluate. To determine the difference in conductivity between a pure and a multicomponent system, RME was used as a biodiesel reference. Figure 4 describes the conductivity curve over the aging time.

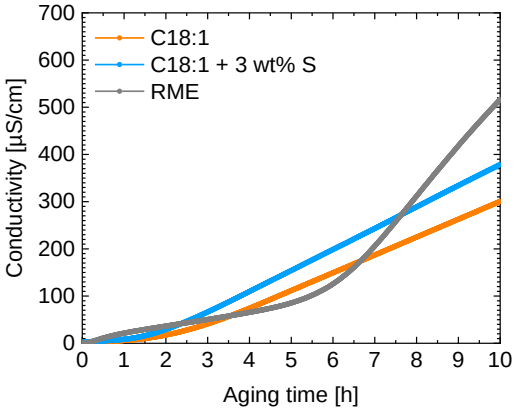

Figure 4. Conductivity of rancimat eluate. To get a first impression on the aging, the C18:1 (orange), C18:1 + 3 wt% S (blue), and RME progress were compared. Every blend of the measurement series illustrated a similar progress, which were more linear compared with common biodiesel.

The measurement shows that both C18:1 blends and RME show a different increase in conductivity. The C18:1 measurements appear to be linear, while RME is more exponential. In addition, the induction time of RME is later. After the induction time, the increase in conductivity is greatest for RME. Compared with the C18:1 blends, the slope of RME was steeper by 0.64 (C18:1) and 0.57 (C18:1 + 3 wt% S). Here, a first dependence of the conductivity on allylic and bis-allylic compounds can be observed. Since the radical stability of these molecules is stronger, the resulting vaporized decomposition products are formed more frequently. It results that the progression of RME is exponential compared with C18:1

trends. The influence of solketal leads to a stronger slope compared with pure C18:1 (0.17). Overall, it can be seen that the kinetics of the mixtures are different. The next step was to determine the time dependence of the disappearance of 3 wt% S using GC-MS. Figure 5 shows the time progression of the solketal content.

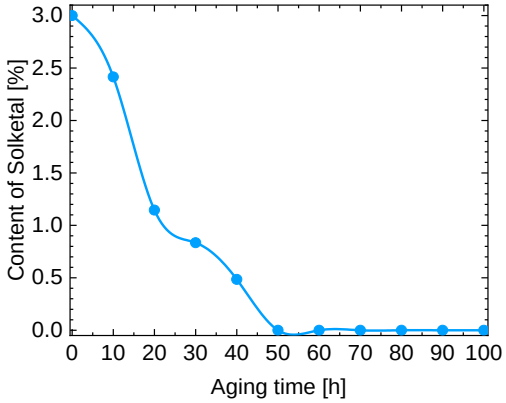

Figure 5. Development of solketal content of the C18:1 + 3 wt% S blends over time by using GC–MS. Number of measurements (n = 2).

Solketal is no longer detectable starting at 50 hours due to degradation. Solketal therefore decomposes in the period between 40–50 h. This means that at this point, the interaction between the components is no longer directly influenced by the solketal and therefore, the chemical and physical environment changes, thus the interactions change. The strongest degradation of solketal occurs in the first 20 hours. However, the aged products of solketal aging can still interact with C18:1. Nevertheless, the specific time of 40 h should be considered in further studies (e.g., peroxide value). One possibility is that another aging mechanism could take place due to the decomposition of solketal. Solketal and its solubility property may affect kinetics, resulting in a time shift compared with pure C18:1. In addition, solubility may affect the degree of the aging of biodiesel. To evaluate the degree of the aging of biodiesel, the kinematic viscosity was plotted for C18:1 and C18:1 + 3 wt% S blends (Figure 6).

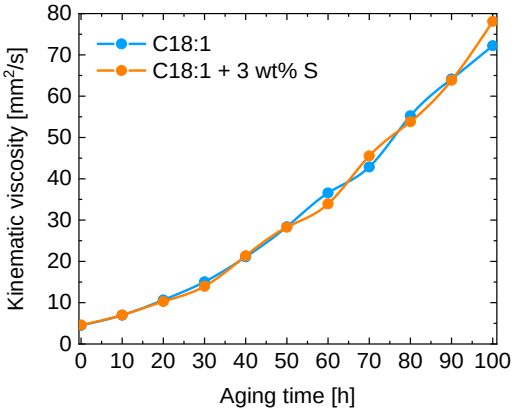

Figure 6. Determination of kinematic viscosity (40 °C) progress over time (0–100 h). The viscosity is compared between C18:1 (blue line) and C18:1 + 3 wt% S (orange line) (n = 2).

Both blends confirm the exponential increase in kinematic viscosity measurements due to fuel aging [28]. During 0–50 h, the plots are similar, indicating no significant effect of 3 wt% solketal. This correlates with the observation of solketal content over time, which describes that solketal is still in solution during this period. However, between 60 and 70 h, a crossover occurs that leads to a different evolution of kinematic viscosity. This can be

interpreted as a change in aging behavior. Considering the aging products formed due to decomposition, it is necessary to determine the total value of peroxides. The reason for this is that peroxides are formed first. The repeat measurements of the peroxide value were plotted in individual graphs. The purpose of this is to be able to assess the progressions and correlations more accurately (Figures 7 and 8).

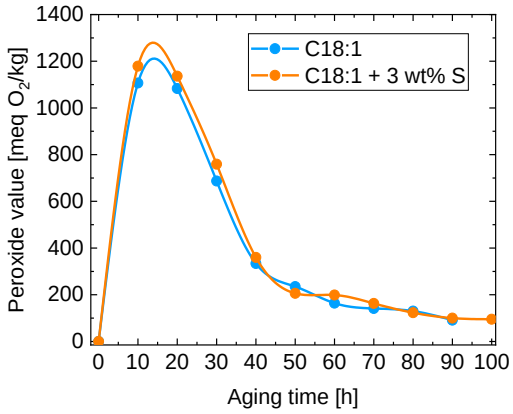

Figure 7. Determination of first measurement peroxide values over time (0–100 h) according to wheeler. The blue line describes the pure C18:1 and the orange line the C18:1 + 3 wt% S.

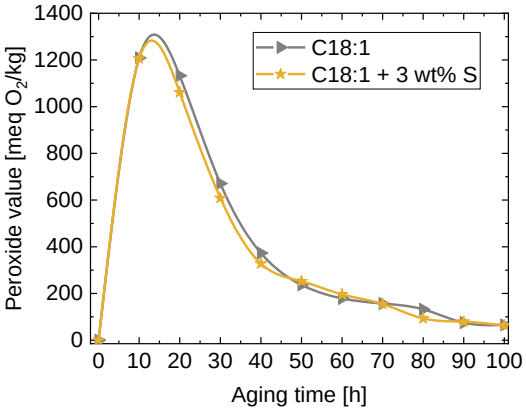

Figure 8. Determination of second measurement peroxide values over time (0–100 h) according to wheeler. The silver line describes the pure C18:1 and the yellow line the C18:1 + 3 wt% S.

The graphs show that the formation of peroxides occurs in the first 10 hours. In general, the peroxide value of pure C18:1 is higher than the peroxide value of normal biodiesel, indicating the formation of more stable peroxides (Figures 9 and 10) [29,30]. Thereafter, decomposition begins up to 40 hours, where the curve flattens and degradation decreases. The fact that degradation of peroxides occurs further after 10 hours is related to the stability of the peroxides under thermo-oxidative conditions. At these conditions, the reactivity of the peroxides is too high [31]. Other aging products are not formed to any significant extent during the first 10 hours. In addition, crossovers between 40–50 h and 50–60 h are observed to occur earlier compared with the kinematic viscosity transition, confirming its role as a precursor. More deeply, it is described that peroxides are the precursors of epoxides, another group of oxidized aging products. To investigate this hypothesis, the correlation of peroxide and epoxide values was observed. Considering the reproducible peroxide measurements, the trend of epoxide values should also follow a similar tendency. Figures 11 and 12 show the progress of epoxides over the aging time of the two series of measurements. The epoxides were determined by GC–MS.

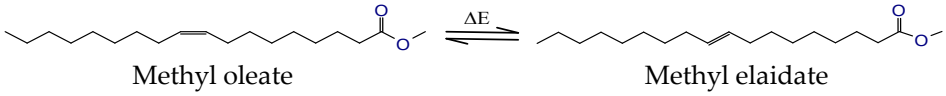

Figure 9. Energy dependent cis-trans isomerization of methyl oleate and methyl elaidate. This mechanism is declared as a possibility as to how the trans-9,10-epoxide could be formed.

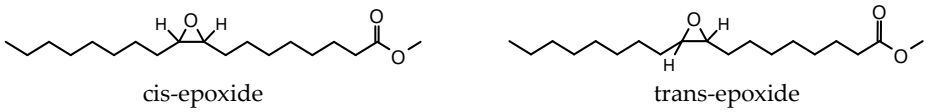

Figure 10. Chemical structure of cis-epoxide (left) and trans-epoxide (right). The steric is determined by the hydrogens [17,32,33].

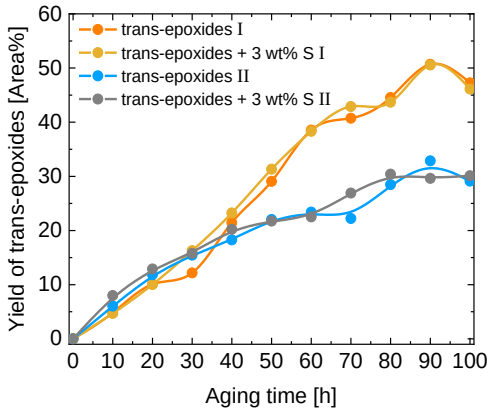

Figure 11. GC–MS measurement to record the yield of trans-epoxide while aging the blends over time. On the one hand, the orange line (C18:1) and the yellow line (C18:1 + 3 wt% S) represent the first measurement. On the other hand, the blue line (C18:1) and silver line (C18:1 + 3 wt% S) depict the repeat measurement (n = 2). I describes the first, II the second measurement.

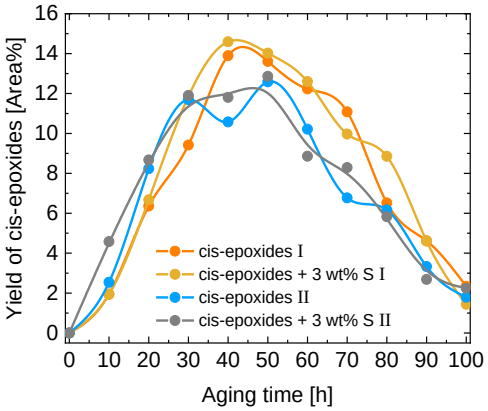

Figure 12. GC–MS measurement to record the yield of cis-epoxide while aging the blends over time. On the one hand, the orange line (C18:1) and the yellow line (C18:1 + 3 wt% S) represent the first measurement. On the other hand, the blue line (C18:1) and silver line (C18:1 + 3 wt% s) depict the repeat measurement (n = 2). I describes the first, II the second measurement.

The experimental setup can be used to detect both cis- and trans-methyl esters and epoxides. Isomerization of fatty acids by thermal energy input has been described in the literature, including rancimate conditions [34,35]. Emken described that cis-trans isomerization can also occur during biodiesel aging, and cis- and trans-epoxides are formed [17,36]. The stereochemistry of epoxide is determined by the stereochemistry of alkene, which means that the acid-based epoxides are mostly cis-epoxides [37]. However, due to the

occurrence of cis-trans isomerization under these conditions, a small percentage of trans-epoxides could also be formed by acids. Mainly, the trans-epoxides are formed by the autoxidative process at the C8 and C11 positions [38]. From 0–40 h, both epoxide isomers tend to show more epoxides for C18:1 + 3 wt% solketal. This indicates that epoxidation occurs more strongly in the presence of solketal. In addition, the time course of aging shows that a change in aging occurs starting at 40 hours. This is in agreement with the peroxide values, which also show a change after 40 h. In particular, the trend of the trans-epoxides of the two measurements shows a similar course up to 40 h. After 40 h, the two measurements move into different quantity ranges and then show a difference of up to 15%. Although the measurements run into different quantity ranges, C18:1 and C18:1 + 3 wt% S show a similar correlation when compared with each other. For the cis-epoxides, the crossover between 60 and 70 h is also observed. For the trans-epoxides, the crossover is weak. For the cis-epoxides, a buildup of molecules is observed up to 40 h, followed by degradation. It is noticeable that after 40 h, further reactions of the cis-epoxides take place. Due to sterics and the associated greater ring tension, cis-epoxides are more reactive [39]. In addition, the course of the trans-epoxides after 40 h may also possibly be related to decomposition, which, however, proceeds at different rates. This enhanced onset of degradation from 40 h can help identify epoxide-related degradation products in the sequence, which are thus detected only from 50 h onward. Nevertheless, epoxide precursors suggest that the peroxides are not the direct precursors of the epoxides, considering the different progressions. Another possible precursor could be aging products that have acid functionality (e.g., a carboxyl group). This functionality is expressed by the acid value. By increasing the acid value, enhanced interaction with unaged C18:1 molecules can occur. Figure 13 shows the acid value graphs for the two measurements.

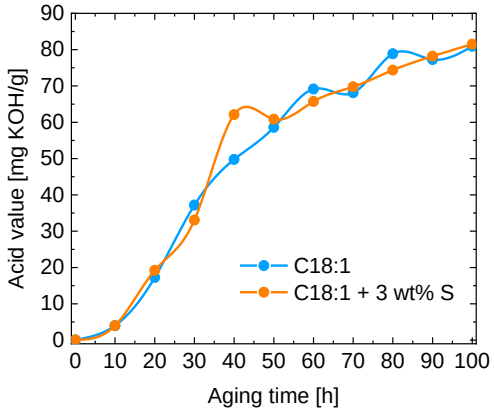

Figure 13. Comparison of acid value over aging time of C18:1 (blue) and C18:1 + 3 wt% S (orange) by using titration method according to EN 14,104 (n = 2).

Between 0 and 50 hours, the trend of C18:1 + 3 wt% S is higher, except for the 30-hour measurement. The trend shows a greater correlation with epoxide evolution than that of peroxides. After 50 h, several crossovers occur, supporting the hypothesis of a mechanistic change. The obtained parameters show consistent data considering the influence and effect of solketal and the possibility of kinetic change already discussed. The correlation between peroxides, acids, and epoxides indicates that acids are precursors for epoxides. However, decomposition of epoxides generates new products and affects the number of epoxides. One class of products are ketones, e.g., methyl 9-oxooctadecanoate and methyl 10-oxooctadecanoate. They are generated by a rearrangement reaction (see Figure 14) [40].

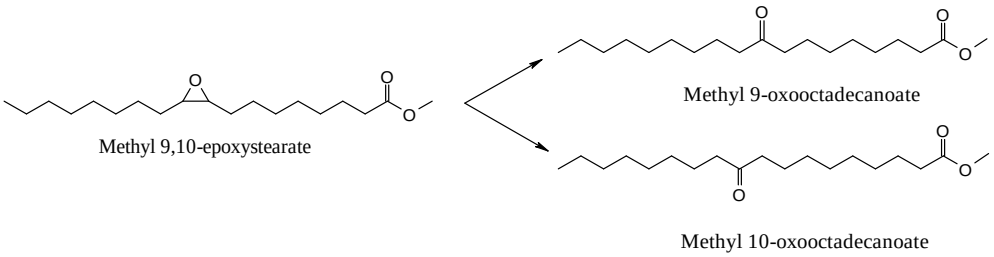

Figure 14. Rearrangement of epoxides to generate two ketone isomers (Methyl 9-oxo- and 10-oxo-stearic acid) [41].

It is observed that the onset of formation of methyl 9-oxooctadecanoate begins after 40 h, which is consistent with the degradation of cis- and trans-epoxides (Figure 15). The degradation of epoxides also affects changes in aging behavior due to the formation of a new molecule. A crossover is observed at later aging times (80–90 h). The trend of C18:1 + 3 wt% S tends to lead to higher yields. As more epoxides are formed in solketal mixtures, more ketones are also formed, which has an effect on total epoxides. However, the reproducibility of the measurement of ketones is difficult because they are the fourth aging product (C18:1 → peroxide → acid → epoxide → ketone). Nevertheless, direct formation of methyl 9-oxooctadecanoate from peroxides is also possible [29]. Looking at the peroxide trends, no significant effect of solketal on the peroxide value can be seen, indicating that the epoxide mainly serves as a precursor for ketones.

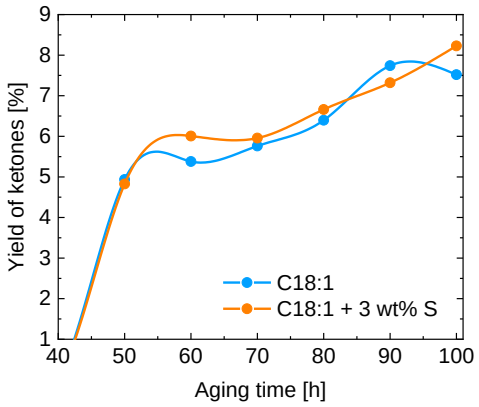

Figure 15. Development of 9-oxooctadecanoate over aging time. The progress of ketones was determined for C18:1 (blue) and C18:1 + 3 wt% S (orange) (n = 2).

4. Conclusions

In general, kinetic studies showed that a change in aging can be implied by 3 wt% solketal. In addition, the time evolution of aging was shown, leading to a better understanding of the sequence of aging products and the influence of solketal. It was possible to define more precisely which products were related to C18:1 and solketal. The first observation was that there was a different boiling behavior between RME and C18:1 under these aging conditions. This is the result of less short-chained decomposition products. From the time of decomposition of solketal, the kinematic viscosity curve changed, and crossovers occurred. These crossovers were consistent with other parameters studied, such as the aging products. The aging products showed that there was no direct effect on peroxide formation by solketal. However, the acid and epoxide values showed that more of these functionalities were formed in the presence of solketal. In addition, the time progress showed that the peroxides were formed first and then the acids by decompositions. It was also noticeable that no direct correlation was observed between peroxides and epoxides. The formation of 9-oxooctadecanoate correlated with the decomposition of the cis-epoxide. In summary, the influence of solketal is due to the fact that it generates a higher acid value

in the blends. The fact that it has no influence on the peroxides and it clearly affects the epoxide value indicates that acids are the precursors of epoxides. This is in agreement with the fundamentals and state-of-the-art organic chemistry, which states that epoxidation occurs via peroxy acids as a result of Prileschajew reactions [42]. As a result of autoxidation of aldehydes formed during aging of biodiesel [43,44] as well as oxidized carboxylic acids by peroxides [45,46], in-situ peroxyacids are possible. Due to the late build-up of ketones and the correlation of the degradation of epoxides, the following sequence can be observed: Peroxide → Acid/Aldehydes → Epoxide → Ketone.

5. Outlook

Simplification of the system has led to an estimation of how C18:1 behaves as a pure substance and in the mixture with solketal during aging. Next, the system should be extended, and the complexity increased. More specifically, it would be useful to perform the same studies with methyl linoleate (C18:2) and methyl linolenate (C18:3). This would allow for the influence of allylic and bis-allylic double bonds to be determined. Furthermore, the amounts of solketal should be varied, as different amounts may also provide further additional insight. In addition to chemical fuel aging, the physical interactions between aged biodiesel and, for example, engine oil should be further investigated. Due to the dilution of engine oil, this issue is particularly critical [47]. Regarding the confirmation of the position of the trans-9,10-epoxide, further characterization should be conducted.

Author Contributions: Conceptualization, investigation, validation, data curation, writing original draft, formal analysis, J.T.; Conceptualization, investigation, validation, methodology, F.S.; Conceptualization, investigation, validation, L.A.; Writing—review and editing, conceptualization, A.L.; Writing—review and editing, project administration, funding acquisition, R.T.; Writing—review and editing, supervision, W.R.; Writing—review and editing, supervision, conceptualization, investigation, project administration, J.K. All authors have read and agreed to the published version of the manuscript.

Funding: This research received no external funding.

Data Availability Statement: The data presented in this study are available upon request from the corresponding author. The data are not publicly available due to policy.

Conflicts of Interest: The authors declare no conflict of interest.

References

1. Ramos, M.J.; Fernández, C.M.; Casas, A.; Rodríguez, L.; Pérez, Á. Influence of fatty acid composition of raw materials on biodiesel properties. *Bioresour. Technol.* **2009**, *100*, 261–268. [CrossRef] [PubMed]
2. Fang, H.L.; McCormick, R.L. *Spectroscopic Study of Biodiesel Degradation Pathways*; SAE Technical Paper; SAE: Warrendale, PA, USA, 2006.
3. Tuerck, J.; Singer, A.; Lichtinger, A.; Almaddad, M.; Türck, R.; Jakob, M.; Garbe, T.; Ruck, W.; Krahl, J. Solketal as a renewable fuel component in ternary blends with biodiesel and diesel fuel or HVO and the impact on physical and chemical properties. *Fuel* **2022**, *310*, 122463. [CrossRef]
4. Hamacher, D.; Schrader, W. Investigating Molecular Transformation Processes of Biodiesel Components During Long-Term Storage Via High-Resolution Mass Spectrometry. *ChemSusChem* **2022**, *15*, e202200456. [CrossRef] [PubMed]
5. Krahl, J.; Petchatnikov, M.; Schmidt, L.; Munack, A.; Bünger, J. *Spektroskopische Untersuchungen zur Ergründung der Wechselwirkungen zwischen Biodiesel und Dieselkraftstoff bei Blends*; Braunschweig und Coburg: Braunschweig, Germany, 2009.
6. Singer, A.; Schröder, O.; Pabst, C.; Munack, A.; Bünger, J.; Ruck, W.; Krahl, J. Aging studies of biodiesel and HVO and their testing as neat fuel and blends for exhaust emissions in heavy-duty engines and passenger cars. *Fuel* **2015**, *153*, 595–603. [CrossRef]
7. Frankel, E. *Lipid Oxidation*; The Oily Press: Dundee, Scotland, 1998; Volume 13.
8. Kim, H.J.; Min, D.B. 11. Chemistry of Lipid Oxidation. *Food Lipids Chem. Nutr. Biotechnol.* **2008**, *1*, 299.
9. Stuhr, R.; Bayer, P.; von Wangelin, A.J. The Diverse Modes of Oxygen Reactivity in Life & Chemistry. *ChemSusChem* **2022**, *15*, e202201323.
10. Schaich, K.M. Lipid oxidation: Theoretical aspects. In *Bailey's Industrial Oil and Fat Products*; Wiley: Hoboken, NJ, USA, 2005; Volume 1, pp. 273–303.
11. Min, D.; Boff, J. Chemistry and reaction of singlet oxygen in foods. *Compr. Rev. Food Sci. Food Saf.* **2002**, *1*, 58–72. [CrossRef]
12. Knothe, G. Some aspects of biodiesel oxidative stability. *Fuel Process. Technol.* **2007**, *88*, 669–677. [CrossRef]

13. Regensburger, J. *Spektroskopische Untersuchungen zur Singulett-Sauerstoff-Lumineszenz in Biomolekülen, Bakterien und Zellen*; Universität Regensburg: Regensburg, Germany, 2010.
14. Bär, F.; Knorr, M.; Schröder, O.; Hopf, H.; Garbe, T.; Krahl, J. Rancimat vs. rapid small scale oxidation test (RSSOT) correlation analysis, based on a comprehensive study of literature. *Fuel* **2021**, *291*, 120160. [CrossRef]
15. Romanov, A.N.; Rufov, Y.N.; Korchak, V.N. Thermal generation of singlet oxygen ($^1\Delta_gO_2$) on ZSM-5 zeolite. *Mendeleev Commun.* **2000**, *10*, 116–117. [CrossRef]
16. Kumar, N. Oxidative stability of biodiesel: Causes, effects and prevention. *Fuel* **2017**, *190*, 328–350. [CrossRef]
17. Flitsch, S.; Neu, P.M.; Schober, S.; Kienzl, N.; Ullmann, J.R.; Mittelbach, M. Quantitation of aging products formed in biodiesel during the rancimat accelerated oxidation test. *Energy Fuels* **2014**, *28*, 5849–5856. [CrossRef]
18. Xin, J.; Imahara, H.; Saka, S. Kinetics on the oxidation of biodiesel stabilized with antioxidant. *Fuel* **2009**, *88*, 282–286. [CrossRef]
19. Domingos, A.K.; Saad, E.B.; Vechiatto, W.W.; Wilhelm, H.M.; Ramos, L.P. The influence of BHA, BHT and TBHQ on the oxidation stability of soybean oil ethyl esters (biodiesel). *J. Braz. Chem. Soc.* **2007**, *18*, 416–423. [CrossRef]
20. Türck, J. Kraftstoffe für die Mobilität von morgen. In Proceedings of the Kraftstoffe für die Mobilität von Morgen, 4. Tagung der Fuels Joint Research Group, Dresden, Germany, 10–11 June 2021; Volume 30, pp. 470–477.
21. Mota, C.J.; da Silva, C.X.; Jr, N.R.; Costa, J.; da Silva, F. Glycerin Derivatives as Fuel Additives: The Addition of Glycerol/Acetone Ketal (Solketal) in Gasolines. *Energy Fuels* **2010**, *24*, 2733–2736. [CrossRef]
22. Glassman, I. Soot formation in combustion processes. In *Symposium (International) on Combustion*; Elsevier: Amsterdam, The Netherlands, 1989; Volume 22, pp. 295–311.
23. Bowden, J.; Johnston, A.; Russell, J. *Octane-cetane relationship. Southwest Research In San Antonio TX Belvoir Fuels and Lubricants Research*; Ft. Belvoir: Fairfax County, VA, USA, 1974.
24. Samoilov, V.; Borisov, R.; Stolonogova, T.; Zarezin, D.; Maximov, A.; Bermeshev, M.; Chernysheva, E.; Kapustin, V. Glycerol to renewable fuel oxygenates. Part II: Gasoline-blending characteristics of glycerol and glycol derivatives with C3-C4 alkyl (idene) substituents. *Fuel* **2020**, *280*, 118585. [CrossRef]
25. Moser, B.R. Comparative oxidative stability of fatty acid alkyl esters by accelerated methods. *J. Am. Oil Chem. Soc.* **2009**, *86*, 699–706. [CrossRef]
26. Sabudak, T.; Yildiz, M. Biodiesel production from waste frying oils and its quality control. *Waste Manag.* **2010**, *30*, 799–803. [CrossRef] [PubMed]
27. *ISO 3960:2012*; Animal and Vegetable Fats and Oils—Determination of Peroxide Value—Iodometric (Visual) Endpoint Determination. ISO: Geneva, Switzerland, 2012.
28. Ball, J.C.; Anderson, J.E.; Wallington, T.J. Depolymerization of polyester polymers from the oxidation of soybean biodiesel. *Energy Fuels* **2018**, *32*, 12587–12596. [CrossRef]
29. Canakci, M.; Monyem, A.; Van Gerpen, J. Accelerated oxidation processes in biodiesel. *Trans. ASAE* **1999**, *42*, 1565. [CrossRef]
30. Thompson, J.; Peterson, C.; Reece, D.; Beck, S. Two-year storage study with methyl and ethyl esters of rapeseed. *Trans. ASAE* **1998**, *41*, 931. [CrossRef]
31. Bouaid, A.; Martinez, M.; Aracil, J. Production of biodiesel from bioethanol and Brassica carinata oil: Oxidation stability study. *Bioresour. Technol.* **2009**, *100*, 2234–2239. [CrossRef] [PubMed]
32. Morales, A.; Marmesat, S.; Dobarganes, M.C.; Márquez-Ruiz, G.; Velasco, J. Evaporative light scattering detector in normal-phase high-performance liquid chromatography determination of FAME oxidation products. *J. Chromatogr. A* **2012**, *1254*, 62–70. [CrossRef]
33. Velasco, J.; Marmesat, S.; Bordeaux, O.; Márquez-Ruiz, G.; Dobarganes, C. Formation and evolution of monoepoxy fatty acids in thermoxidized olive and sunflower oils and quantitation in used frying oils from restaurants and fried-food outlets. *J. Agric. Food Chem.* **2004**, *52*, 4438–4443. [CrossRef] [PubMed]
34. Wolff, R.L. Heat-induced geometrical isomerization of α-linolenic acid: Effect of temperature and heating time on the appearance of individual isomers. *J. Am. Oil Chem. Soc.* **1993**, *70*, 425–430. [CrossRef]
35. Cheng, N.; Zhang, J.; Yin, J.; Li, S. Computational and experimental research on mechanism of cis/trans isomerization of oleic acid. *Heliyon* **2018**, *4*, e00768. [CrossRef]
36. Emken, E. cis and trans Analysis of fatty esters by gas chromatography: Octadecenoate and octadecadienoate isomers. *Lipids* **1972**, *7*, 459–466. [CrossRef]
37. Moser, B.R.; Cermak, S.C.; Doll, K.M.; Kenar, J.A.; Sharma, B.K. A review of fatty epoxide ring opening reactions: Chemistry, recent advances, and applications. *J. Am. Oil Chem. Soc.* **2022**, *99*, 801–842. [CrossRef]
38. Frankel, E. Chemistry of free radical and singlet oxidation of lipids. *Prog. Lipid Res.* **1984**, *23*, 197–221. [CrossRef]
39. Cravador, A.; Krief, A. Unusual reactivity of selenoboranes towards epoxides: New selective routes to b-hydroxyselenides and allylalcohols. *Tetrahedron Lett.* **1981**, *22*, 2491–2494. [CrossRef]
40. Wei, Y.; Li, G.; Lv, Q.; Cheng, C.; Guo, H. Epoxidation of methyl oleate and unsaturated fatty acid methyl esters obtained from vegetable source over Ti-containing silica catalysts. *Ind. Eng. Chem. Res.* **2018**, *57*, 16284–16294. [CrossRef]
41. Parker, R.-E.; Isaacs, N. Mechanisms of epoxide reactions. *Chem. Rev.* **1959**, *59*, 737–799. [CrossRef]
42. Saurabh, T.; Patnaik, M.; Bhagt, S.; Renge, V. Epoxidation of vegetable oils: A review. *Int. J. Adv. Eng. Technol* **2011**, *2*, 491–501.
43. Marteau, C.; Ruyffelaere, F.; Aubry, J.-M.; Penverne, C.; Favier, D.; Nardello-Rataj, V. Oxidative degradation of fragrant aldehydes. Autoxidation by molecular oxygen. *Tetrahedron* **2013**, *69*, 2268–2275. [CrossRef]

44. Bravo, A.; Bjorsvik, H.-R.; Fontana, F.; Minisci, F.; Serri, A. Radical versus "oxenoid" oxygen insertion mechanism in the oxidation of alkanes and alcohols by aromatic peracids. New synthetic developments. *J. Org. Chem.* **1996**, *61*, 9409–9416. [CrossRef]
45. Parker, W.E.; Ricciuti, C.; Ogg, C.; Swern, D. Preparation, Characterization and Polarographic Behavior of Longchain Aliphatic Peracids2. *J. Am. Chem. Soc.* **1955**, *77*, 4037–4041. [CrossRef]
46. Greenspan, F.P. The convenient preparation of per-acids. *J. Am. Chem. Soc.* **1946**, *68*, 907. [CrossRef]
47. Thornton, M.J.; Alleman, T.L.; Luecke, J.; McCormick, R.L. Impacts of biodiesel fuel blends oil dilution on light-duty diesel engine operation. *SAE Int. J. Fuels Lubr.* **2009**, *2*, 781–788. [CrossRef]

Disclaimer/Publisher's Note: The statements, opinions and data contained in all publications are solely those of the individual author(s) and contributor(s) and not of MDPI and/or the editor(s). MDPI and/or the editor(s) disclaim responsibility for any injury to people or property resulting from any ideas, methods, instructions or products referred to in the content.